Liquid-Solid Interface Migration at Grain Boundary Regions during Transient Liquid Phase Brazing

K. IKEUCHI, Y. ZHOU, H. KOKAWA, and T.H. NORTH

A two-dimensional (2-D) finite difference model has been used to analyze the effect of grain boundary regions on the migration of the liquid-solid interface during transient liquid phase (TLP) brazing of Ni with Ni-11 wt pct P filler metal. This work has been carried out to explain the differences observed between actual and calculated completion times for isothermal solidification during TLP brazing and the faster isothermal solidification rates when brazing fine-grained nickel-base material. Modeling considers the situation where the grain boundary intersects the liquid-solid interface at right angles. Four factors are considered in addition to solute diffusion in solid and liquid phases, *viz.*, (1) high diffusivity at the grain boundary region, (2) the balance between the grain boundary energy and the liquid-solid interfacial energy, (3) the interfacial energy due to the curvature of the liquid-solid interface, and (4) diffusional flow along the liquid-solid interface (produced by the gradient of solute chemical potential resulting from factors (2) and (3)). Increased solute diffusivity at the grain boundary region has a negligible effect on migration of the liquid-solid interface in the bulk region and shifts the interface at the grain boundary region in a direction opposite that observed in actual brazed samples. On the other hand, when factors (2) through (4) above are taken into account, the liquid-solid interface in the region of the grain boundary is displaced in the same direction as in the experimental results and liquid penetration comparable with the experimental results occurs at the grain boundary region. Factors (2) through (4) accelerate the isothermal solidification process in the bulk region in accordance with actual experimental test results.

I. INTRODUCTION

IN transient liquid phase (TLP) brazing, the filler metal is placed between the base metal surfaces and the joining operation is carried out at a temperature between the liquidus of the filler and the solidus of the base metal.[1] On holding at the brazing temperature, solute elements in the filler metal diffuse into the base metal and dissolution occurs prior to isothermal solidification. The rate-controlling factors which determine dissolution and isothermal solidification have been examined in a number of theoretical and experimental studies and the time for completion of the TLP brazing operation has been estimated.[2-8]

In a previous study,[4] liquid-solid interface migration during TLP brazing of commercially pure nickel using a Ni-11 wt pct P filler metal was investigated using one-dimensional (1-D) computer modeling. The actual isothermal solidification rate in brazed samples was considerably faster than the calculated value, and the disparity between actual and calculated values increased when the base metal grain size decreased.[6,8] An examination of the liquid-solid interface at the grain boundary regions revealed the following:[6]

(a) there was significant liquid penetration at the grain boundaries in the base material, and consequently, the experimental results did not correspond with a key assumption in the 1-D modeling (that the liquid-solid interface would remain planar during the whole brazing cycle[4]);
(b) liquid penetration at the grain boundaries, though undetectable in the dissolution process, was particularly pronounced during the isothermal solidification stage; and
(c) liquid penetration was more pronounced at high angle, random grain boundary regions than at ordered grain boundaries (small angle and twin boundaries).

It is important to point out that Tuah-Poku *et al.*[5] had already suggested that the liquid penetration at grain boundary regions produced the marked difference between their calculated and experimental completion times for isothermal solidification during TLP brazing of silver using copper filler metal.

II. PRIOR WORK

Several reports have dealt with liquid penetration at grain boundary regions, although none is directly applicable to the TLP brazing situation. Mullins[9,10] examined grain boundary grooving when a bicrystal contacted a surrounding fluid (liquid or gas) that was saturated with the solid element. The initial fluid-solid interface was flat, and the grain boundary region intersected the interface at right angles (Figure 1). Mullins made several assumptions in his analysis, namely,

(1) that the fluid-solid interface energy was independent of crystallographic orientation,
(2) that the Gibbs-Thompson equation determined the relation between fluid-solid interface curvature and chemical potential,

K. IKEUCHI and H. KOKAWA, formerly Visiting Scientists, Department of Metallurgy and Materials Science, University of Toronto, are Associate Professors with the Welding Research Institute, Osaka University, Osaka, Japan, and with the Department of Materials Processing, Tohoku University, Sendai, Japan, respectively. Y. ZHOU, Graduate Student, and T.H. NORTH, WIC/NSERC Professor, are with the Department of Metallurgy and Materials Science, University of Toronto, Toronto, ON M5S 1A4, Canada.

Manuscript submitted February 10, 1992.

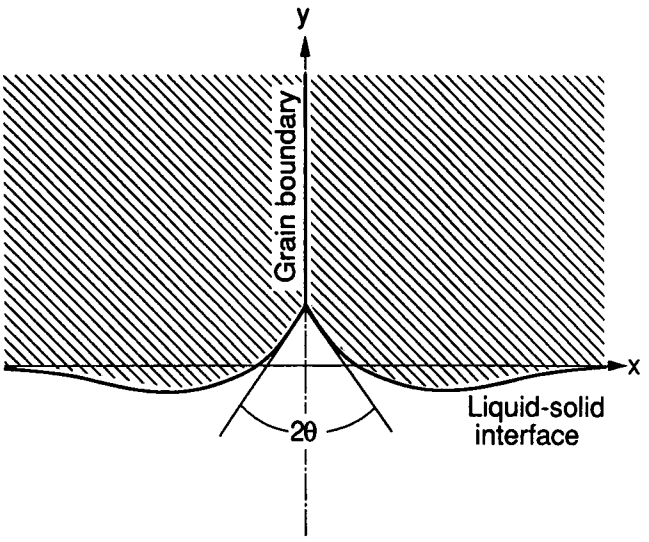

Fig. 1 — Schematic illustrating the grain boundary grooving.

(3) that quasi-steady-state volume diffusion occurred in the fluid,
(4) that the slope of the interface changed little from the initial interface configuration, and
(5) that there was negligible convection in the fluid.

In a gas-solid system, the grain boundary grooving occurred due to a combination of interface diffusion and evaporation-condensation.[9] In a liquid-solid system, grain boundary grooving occurred mainly due to volume diffusion in the saturated fluid.[10]

Based on assumption (3), the concentration of solid element $c^f(x,y,z)$ in the liquid satisfies the relation

$$\nabla^2 c^f(x,y,t) = 0 \qquad [1]$$

Assumption (4) means that the interface can be represented as the plane $y = 0$. From assumption (2), therefore, the boundary condition at the interface is given by the relation

$$c^f(x,0,t) = c_0^f \cdot \left\{1 + \frac{E_s \cdot \Omega}{R \cdot T} \cdot K(x,t)\right\} \qquad [2]$$

where c_0^f is the concentration of solid element in the liquid phase in equilibrium with the flat interface, Ω is the atomic volume of the solid atom, E_s is the liquid-solid interfacial energy, and K is the curvature of the interface (the concentrations of c^f and c_0^f are expressed as the number of atoms per unit volume). The curvature K is given as

$$K = \frac{\dfrac{\partial^2 Y}{\partial x^2}}{\left(1 + \left(\dfrac{\partial Y}{\partial x}\right)^2\right)^{3/2}} \qquad [3]$$

Because of assumption (4), $\partial Y/\partial x \ll 1$ and K can be approximated by

$$K = \frac{\partial^2 Y}{\partial x^2} \qquad [4]$$

Mullins[9,10] evaluated the concentration distribution of $c^f(x,y,z)$ by solving Eq. [1] using the boundary condition given in Eq. [2].

If interdiffusion in the solid is negligible, the rate of migration of a segment of the interface will depend on volume diffusion only in the liquid phase, namely,

$$\frac{\partial Y}{\partial t} = D_l \cdot \Omega \cdot \left(\frac{\partial c^f}{\partial y}\right)_{y=0} \qquad [5]$$

where $Y(x,t)$ is the y-coordinate at the interface and D_l is the interdiffusion coefficient in the liquid phase. Mullins[9,10] differentiated this equation twice with respect to x to express Eq. [5] in terms of interface curvature:

$$\frac{\partial K}{\partial t} = D_l \cdot \Omega \cdot \frac{\partial^2}{\partial x^2}\left[\left(\frac{\partial c^f}{\partial y}\right)_{y=0}\right] \qquad [6]$$

Substituting the concentration distribution $c^f(x,y,z)$ which satisfies the boundary condition in Eq. [2] produced an integrodifferential equation for $K(x,t)$. This equation was solved analytically, assuming that the interface had a fixed slope at $x = 0$ given by

$$\left(\frac{\partial Y}{\partial x}\right)_{x=0} = -\cot\theta \qquad [7]$$

The dihedral angle θ (Figure 1) is determined by the well-known equation for the balance between the grain boundary energy E_g and the interface energy E_s,[11]

$$E_g = 2E_s \cos\theta \qquad [8]$$

Based on these calculations, Mullins found that the groove profile had a fixed shape and linear dimensions that were proportional to $(\text{time})^{1/3}$.

Steidel *et al.*[12] extended Mullins'[9,10] analysis to the case where the small slope approximation (Eq. [4]) was not valid. Since $(\partial Y/\partial X)$ was no longer negligible, they used Eq. [3] to express the curvature K. Finally, they used numerical calculation to estimate the activation energy for diffusion (by comparing the calculated results with the experimental results) and suggested a possible method for evaluating the liquid-solid interfacial energy.

Vogel and Ratke[13] took account of grain boundary diffusion in a recent article that examined grain boundary grooving when solid aluminum contacted a liquid Al-In alloy. Their approach was similar to that indicated by Mullins,[9,10] except that grain boundary diffusion was taken into account. However, there are problems with this approach.

(a) When calculating the solute concentration in the liquid phase due to the grain boundary diffusion, they did not consider that indium depletion in the liquid phase near the grain boundary caused the migration of the liquid-solid interface. Since the concentrations of the liquid and solid phases are in equilibrium and indium lowers the liquidus temperature of the aluminum, the liquid interface will migrate in the direction of the bulk liquid.
(b) They applied Eq. [6] to the whole system. Since this equation was derived based on the assumption that there was negligible diffusional flow in the solid, this equation cannot be applied to the grain boundary region if grain boundary diffusion is substantial.

(c) Their calculations violated the thermodynamic equilibrium condition at the liquid-solid interface, and they extended the limited slope approximation beyond its application limit.

The Mullins'[9,10] grain boundary grooving approach cannot be applied to liquid-solid interface migration during TLP brazing, because it considers negligible solute diffusion in solid and a saturated liquid phase, namely, a situation where no diffusional flow occurs in the liquid and solid phases unless interface curvature exists or there is a point of grain boundary intersection with the liquid-solid interface. In this case, a flat interface that has no intersection with a grain boundary will not migrate. In direct contrast, during TLP brazing, diffusional flow caused by the concentration gradient in the liquid and solid phases brings about migration of the liquid-solid interface, even if the interface is flat and there is no grain boundary intersection. The present study uses computer modeling to estimate the effect of grain boundary regions on migration of a flat liquid-solid interface produced during TLP brazing of nickel using Ni-11 wt pct P filler metal.

III. COMPUTER SIMULATION

In order to account for the effect of grain boundary regions on the TLP brazing process, we must solve a two-dimensional (2-D) or three-dimensional (3-D), nonsteady-state diffusion problem involving a change of phase. A number of numerical analyses have been reported concerning 2-D and 3-D problems involving a change of phase.[14,15,16] However, to our knowledge, none has dealt with the problem using boundary conditions which allow for the influence of the grain boundary on liquid-solid interface migration. Because of this, we have developed model, formulation, and numerical analyses which simulate migration of the liquid-solid interface in the region of the grain boundary during TLP brazing.

A. *Model*

In the actual brazing situation, grain boundaries are not planar and they intersect the liquid-solid interface at different angles and at different intervals. Since it is extremely difficult to solve a problem with such a complicated grain boundary configuration, we have examined the simpler, 2-D situation illustrated in Figure 2. In this case, the grain boundaries are assumed to be planar and parallel to each other, they are perpendicular to the initial liquid-solid interface at a constant interval, and they are symmetrically arranged with respect to the y-axis and x-axis (the centerline of the filler metal). The chemical composition and the coordinates of the liquid-solid interface for this system are obtained by solving the diffusion equations for the shadowed area shown in Figure 2.

The following assumptions are made for mathematical simplification.

(1) The diffusion coefficient, molar volume, and activity coefficient of the solute are independent of composition in the liquid and solid phases. The molar volume of the liquid phase is the same as that of the solid.
(2) Flow of liquid as a result of convection and stirring is negligible, and hence, the movement of solute and solvent elements depends only on diffusion. This assumption seems appropriate, since the width of the liquid phase is around 70 μm at most during TLP brazing.
(3) Local equilibrium between the solid and liquid phases holds everywhere on the liquid-solid interface, and the compositions of the liquid and solid phases on the interface are given by the liquidus and solidus lines in the equilibrium phase diagram.
(4) No intermediate phases are formed during the joining operation.
(5) The Kirkendall effect is neglected.

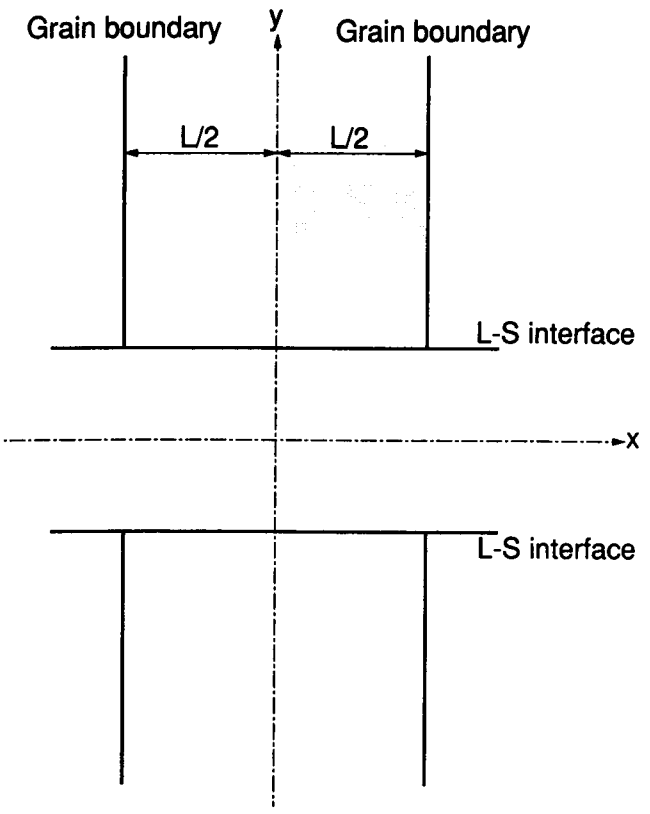

Fig. 2—Grain boundary/liquid-solid interface model used in calculations.

The following factors are important at the grain boundary region:
(1) grain boundary diffusion;
(2) the balance between the grain boundary energy and the liquid-solid interfacial energy;
(3) grain boundary solute segregation;
(4) grain boundary impurity segregation; and
(5) the difference in the melting points of the grain boundary and the bulk region.

Since it is difficult to take into account all the above factors, the present article emphasizes the influence of high solute diffusivity at the grain boundary region and the balance between the grain boundary energy and the liquid-solid interfacial energy. These particular factors are selected, since we assume the following.

(a) Migration of the liquid-solid interface depends markedly on interdiffusion.
(b) Liquid penetration at grain boundary regions is essentially determined by the balance between the grain

boundary energy and the liquid-solid interfacial energy, as suggested by previous articles[9–13] dealing with grain boundary grooving.

Thus, our calculations allow for solute diffusion in the bulk solid and liquid phases, the high diffusivity at the grain boundary region, and the balance between the grain boundary energy and liquid-solid interfacial energy.

B. *Formulation*

Using the above assumptions, the change in the composition of the liquid and solid phases at points far from the liquid-solid interface and from the grain boundary can be described as follows:

$$\frac{\partial C_j}{\partial t} = D_j \cdot \nabla^2 C_j \qquad [9]$$

where C_j is the composition of the liquid and solid phases, D_j the interdiffusion coefficient, $j = s$ for the solid phase, and $j = l$ for the liquid phase. In this case, the composition C_j is expressed in the unit of mol fraction.

The migration of the liquid-solid interface can be described by the following equation:

$$(C_l^0 - C_s^0) \cdot \mathbf{V} = -D_l \cdot \frac{\partial C_l}{\partial \mathbf{n}} + D_s \cdot \frac{\partial C_s}{\partial \mathbf{n}} \qquad [10]$$

where $\mathbf{V}$ is the velocity of the interface in the direction normal to the interface, C_l^0 is the liquidus concentration at a brazing temperature, C_s^0 is the solidus concentration, and $(\partial/\partial \mathbf{n})$ is the directional differential normal to the interface. According to an analysis by Patel,[17] Eq. [10] can be transformed as follows:

$$(C_l^0 - C_s^0) \cdot \frac{\partial Y}{\partial t} = \left\{ -D_l \cdot \left(\frac{\partial C_l}{\partial y} \right)_{y=Y} + D_k \cdot \left(\frac{\partial C_s}{\partial y} \right)_{y=Y} \right\} \cdot \left\{ 1 + \left(\frac{\partial Y}{\partial x} \right)^2 \right\} \qquad [11]$$

where $Y(x, t)$ is the y-coordinate of the liquid-solid interface, $k = s$ for the bulk region, $k = g$ for the grain boundary region, and D_g is the grain boundary diffusion coefficient. This equation gives the velocity of the liquid-solid interface in the y-direction. Therefore, by using this equation, we can calculate the migration of the liquid-solid interface along grid lines which are parallel to the y-axis (this is the basis of the finite difference analysis described in Section III–C).

The concentration at the grain boundary is given by[18]

$$\frac{\partial C_b}{\partial t} = -2 \cdot \frac{D_s}{X_b} \cdot \left(\frac{\partial C_s}{\partial x} \right)_{x=X_b/2} + D_g \cdot \frac{\partial^2 C_b}{\partial y^2} \qquad [12]$$

where C_b is the concentration at the grain boundary region, D_g is the interdiffusion coefficient at the grain boundary region, and X_b is the width of the grain boundary region.

The boundary and initial conditions employed are as follows:

$$\frac{\partial C_l}{\partial y} = 0 \qquad \text{for } t > 0 \text{ and } y = 0$$

$$\frac{\partial C_l}{\partial x} = \frac{\partial C_s}{\partial x} = 0 \qquad \text{for } t > 0 \text{ and } x = 0$$

(on the symmetry axis)

$$C_s = 0 \qquad \text{for } t > 0 \text{ and } y = \infty$$

$$C_s = 0 \qquad \text{for } t = 0 \text{ and } y \geq h/2$$

$$C_l = C_f \qquad \text{for } t = 0 \text{ and } h/2 \geq y \geq 0$$

$$Y = h/2 \qquad \text{for } t = 0$$

where h and C_f are the thickness and concentration of the filler metal, respectively.

1. *Balance between the grain boundary energy and the liquid-solid interfacial energy*

Suppose that a grain boundary intersects a liquid-solid interface at point O and that the intersecting point shifts from O to O′ by ΔY, as shown in Figure 3. The change in free energy caused by this shift of the intersecting point is given by[19]

$$\Delta G \approx (-E_g + 2 \cdot E_s \cdot \cos \phi) \cdot \Delta Y \qquad [13]$$

where E_g is the grain boundary energy, E_s is the liquid-solid interfacial energy, and the orientation dependence of E_s is assumed to be negligible. The thickness of the specimen in the direction perpendicular to the plane of the page is assumed to be the unit length in Figure 3.

From Eq. [13], the solute at the intersecting point O has an excess chemical potential, $\Delta\mu$, compared with the solute in the bulk, given by the following equation:

$$\Delta\mu = \frac{\Delta G}{\Delta n} = (-E_g + 2 \cdot E_s \cdot \cos \phi) \frac{\Delta Y}{\Delta n} = (-E_g + 2 \cdot E_s \cdot \cos \phi) \frac{\bar{V}}{(C_l^0 - C_s^0) \cdot \delta} \qquad [14]$$

where Δn(mol) is the amount of solute required to shift the intersecting point from O to O′, $\bar{V}$ the molar volume of the liquid and solid phases, and δ the width over which

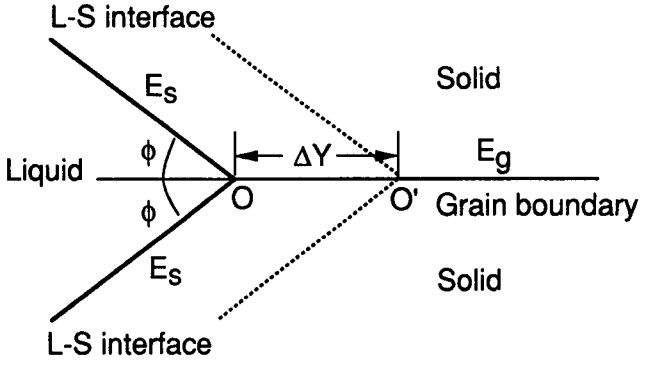

Fig. 3—Schematic illustrating the point of intersection of the grain boundary with the liquid-solid interface.

the chemical potential of the solute is influenced by the grain boundary. In the present calculation, δ is taken to be equal to the grid size in the x-direction, ε.

In order to take into account the effects of the chemical potential, $\Delta\mu$, on solute diffusion, we introduce equivalent concentrations at the intersecting point C_l^e and C_s^e given by the following equations:

$$C_l^e \approx C_l^0 \cdot \left(1 + \frac{\Delta\mu}{RT}\right) \quad [15]$$

and

$$C_s^e \approx C_s^0 \cdot \left(1 + \frac{\Delta\mu}{RT}\right) \quad [16]$$

2. *Interfacial energy due to the curvature of the liquid-solid interface*

The curvature of the liquid-solid interface resulting from liquid penetration at the grain boundary also influences the chemical potential of the solute. The solute at the liquid-solid interface having curvature radius r has an excess chemical potential, $\Delta\mu$, compared with that of the bulk solute, expressed as[20]

$$\Delta\mu = -\frac{E_s}{r} \cdot \frac{\bar{V}}{C_l^0 - C_s^0} \quad [17]$$

The influence of this excess chemical potential on solute diffusion is taken into account by introducing the equivalent concentrations C_l^e and C_s^e given by

$$C_l^e \approx C_l^0 \cdot \left(1 + \frac{\Delta\mu}{RT}\right) \quad [18]$$

and

$$C_s^e \approx C_s^0 \cdot \left(1 + \frac{\Delta\mu}{RT}\right) \quad [19]$$

3. *Diffusion along the liquid-solid interface*

As can be seen from Eqs. [14] and [17], the grain boundary energy and the liquid-solid interfacial energy produce a chemical potential gradient along the liquid-solid interface. This gradient of the chemical potential causes diffusional flow along the liquid-solid interface and, consequently, gives rise to migration of the liquid-solid interface described by[9]

$$\frac{\partial Y}{\partial t} = \frac{D_i \cdot C_i \cdot w}{RT(C_l^0 - C_s^0)} \cdot \frac{\partial}{\partial x}\left[\left\{1 + \left(\frac{\partial Y}{\partial x}\right)^2\right\}^{-1/2} \cdot \frac{\partial \Delta\mu}{\partial x}\right] \quad [20]$$

where D_i is the diffusion coefficient along the liquid-solid interface, C_i is the composition of the liquid-solid interface, and w is the thickness of the liquid-solid interface. The composition C_i is taken as $(C_l^0 + C_s^0)/2$. The migration rate of the interface is assumed to be the sum of the migration rates given by Eqs. [11] and [20].

C. *Numerical Analysis*

In the present investigation, the diffusion equations described in the preceding section are solved numerically using the explicit finite difference method. As shown in Figure 4, a network of lines is passed through the shadowed area in Figure 2. The interval between the lines parallel to the y-axis is ε. The intervals between the lines parallel to the x-axis are ξ for $3h \geq y \geq 0$ and ξ' $(=5\xi)$ for $y \geq 3h$. The compositions of nodes far from the liquid-solid interface and grain boundary region are computed using the finite difference expression for Eq. [9].

In order to estimate the composition of the grain boundary region using the finite difference expression for Eq. [12], we must employ a grid size, ε, as small as the width of the grain boundary region, $X_b(\sim 10^{-9}$ m). However, when such a small ε value is employed, it takes an extremely long calculation time to obtain calculated values comparable with actual experimental results. Therefore, we have estimated the average composition of the grain boundary region and its vicinity, using effective diffusion coefficients D_g^x in the x-direction and D_g^y in the y-direction:

$$D_g^x = \frac{\varepsilon + X_b}{\frac{\varepsilon}{D_s} + \frac{X_b}{D_g}} \approx D_s \quad [21]$$

and

$$D_g^y = \frac{\varepsilon \cdot D_s + X_b \cdot D_g}{\varepsilon + X_b} \quad [22]$$

These diffusion coefficients are derived from the effective diffusion coefficients of a laminate composite comprising layers of different properties sandwiched together, where D_g^y is the diffusion coefficient in the direction parallel to the layers and D_g^x in the direction perpendicular to the layers.[21] Using these diffusion coefficients, the

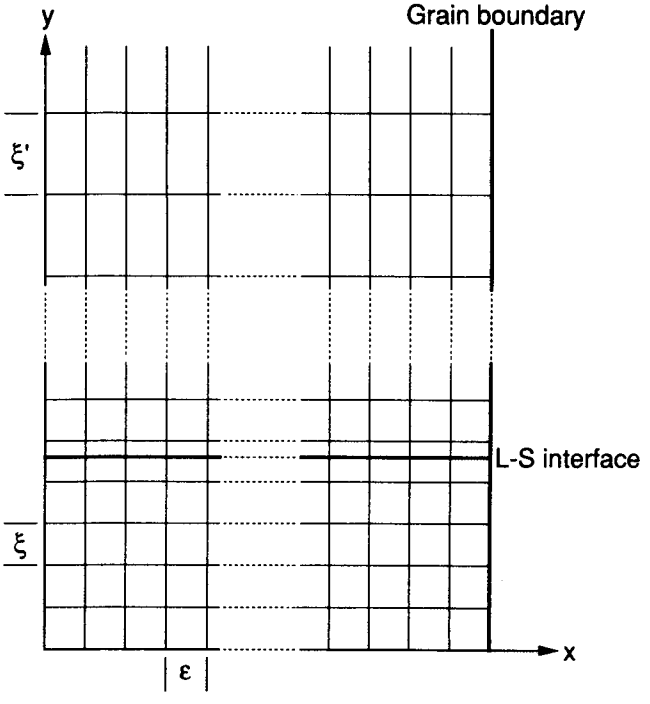

Fig. 4—Finite difference grid used.

composition change, ΔC_b, of nodes at the grain boundary region for a time difference Δt can be expressed as

$$\Delta C_b(m,t) = 2 \cdot D_s \cdot \frac{C_s(n_b - 1, m, t) - C_b(m,t)}{\varepsilon^2} \cdot \Delta t + D_g^y \cdot \frac{C_b(m+1,t) + C_b(m-1,t) - 2 \cdot C_b(m,t)}{\xi^2} \cdot \Delta t \quad [23]$$

where $C_s(n_b - 1, m, t)$ is the composition of the node next to the grain boundary region.

When the liquid-solid interface intersects the nth network line parallel to the y-axis between nodes (n, m) and $(n, m + 1)$, the composition $C_l(n, m)$ of the node adjacent to the liquid-solid interface is given by

$$\Delta C_l(n,m,t) = D_l \cdot \Delta t \left[\left\{ \frac{C_l^e - C_l(n,m,t)}{\Delta \xi} - \frac{C_l(n,m,t) - C_l(n,m-1,t)}{\xi} \right\} \frac{2}{\xi + \Delta \xi} + \frac{C_l(n+1,m,t) + C_l(n-1,m,t) - 2 \cdot C_l(n,m,t)}{\varepsilon^2} \right] \quad [24]$$

where $\Delta \xi$ is the distance between node (n, m) and the liquid-solid interface on the nth network line. The composition change, $\Delta C_s(n, m + 1, t)$, is also estimated in a similar manner.

If diffusion along the liquid-solid interface is neglected, the migration distance, ΔY_1, of the liquid-solid interface is given by the finite difference expression for Eq. [11]:

$$\Delta Y_1(n,t) = \frac{\Delta t}{C_l^0 - C_s^0} \left\{ -D_l \cdot \frac{C_l^e - C_l(n,m,t)}{\Delta \xi} + D_s \cdot \frac{C_s(n,m+1,t) - C_s^e}{\xi - \Delta \xi} \right\} \cdot \left[1 + \left\{ \frac{Y(n+1,t) - Y(n-1,t)}{2 \cdot \varepsilon} \right\}^2 \right] \quad [25]$$

On the other hand, the migration distance of the liquid-solid interface due to diffusion along the liquid-solid interface is given by the finite difference expression for Eq. [20]:

$$\Delta Y_2(n,t) = \frac{B \cdot \Delta t}{\sqrt{1 + Y_x^2}} \left[-\frac{Y_x}{1 + Y_x^2} \frac{Y(n+1,t) + Y(n-1,t) - 2 \cdot Y(n,t)}{\varepsilon^2} \cdot \frac{\Delta \mu(n+1) - \Delta \mu(n)}{2 \cdot \varepsilon} + \frac{\Delta \mu(n+1) + \Delta \mu(n-1) - 2 \cdot \Delta \mu(n)}{\varepsilon^2} \right] \quad [26]$$

where

$$B = \frac{D_i \cdot C_i \cdot w}{RT \cdot (C_l^0 - C_s^0)}$$

and $Y_x = \{Y(n + 1) - Y(n - 1)\}/(2 \cdot \varepsilon)$.

The displacement of the liquid-solid interface, ΔY, for the time difference, Δt is given by

$$\Delta Y = \Delta Y_1 + \Delta Y_2 \quad [27]$$

For the stability of the solution, the time difference Δt is taken as

$$\Delta t < \frac{1}{20} \cdot \frac{\varepsilon^2 \cdot \xi^2}{\varepsilon^2 + \xi^2} \cdot \frac{1}{D_l} \quad [28]$$

The parameters employed in the present study are listed in Table I, and the values of C_l^0, C_s^0, C_f, h, D_l, and D_s are assumed to be the same as those reported in a previous article[4,6] unless otherwise stated.

IV. RESULTS

When the influences of grain boundary diffusion, grain boundary energy, and liquid-solid interfacial energy are ignored, migration of the liquid-solid interface during the TLP brazing is illustrated in Figures 5 and 6. In these figures, the diffusion coefficient in the bulk solid is varied from 1.95×10^{-13} m^2/s[4] by up to 10 times. The vertical axes are the displacement of the liquid-solid

Table I. Parameters Employed in Explicit Finite Difference Modeling

Diffusion coefficient in liquid phase
$D_l = 1.35 \times 10^{-6} \cdot \exp(-9.92 \times 10^4/RT)$ m^2/s
Diffusion coefficient in solid phase
$D_s = 1.0 \times 10^{-6} \cdot \exp(-1.83 \times 10^5/RT)$ m^2/s
Grain boundary diffusion coefficient
$D_g = (1 - 10^5) \times D_s$
Diffusion coefficient along liquid-solid interface
$D_i = 0 - D_l$
Width of grain boundary region
$x_b = 1$ nm
Brazing temperature
$T = 1423$ K
P content of liquidus
$C_l^0 = 0.105$ mol fraction
P content of solidus
$C_s^0 = 0.0138$ mol fraction
Initial concentration of filler metal
$C_f = 0.190$ mol fraction
Initial width of filler metal
$h = 40$ μm
Grain boundary energy
$E_g = 0.35 - 0.848$ Jm^{-2}
L-S interfacial energy
$E_s = 0.35 - 0.848$ Jm^{-2}
Width of L-S interface
$w = 0.3$ nm
Grid size in x direction
$\varepsilon = 2$ μm
Grid size in y direction
$\xi = 5$ μm

interface from its initial position, with increasing width of the liquid phase being positive. As can be seen from Figures 5 and 6, the displacement increases quickly, reaches a maximum in around 10 seconds, and then decreases very slowly. As expected, these results indicate that the time required for completion of the isothermal solidification process is much longer than that for the dissolution process. As can be seen in Figure 6, the plots relating the displacement of the liquid-solid interface with the square root of the holding time approach linearity during the isothermal solidification stage. Also, an increase in the diffusion coefficient in the solid significantly accelerates the isothermal solidification process, although its effect on the dissolution process is relatively weak. On the other hand, an increase in the diffusion coefficient in the liquid phase accelerates the dissolution process, while the isothermal solidification process is only slightly affected.

High solute diffusivity at the grain boundary region alters the profile of the liquid-solid interface, as shown in Figures 7 and 8. In these figures, the displacement of the liquid-solid interface is plotted against the distance from the grain boundary. In each curve, the area below the curve is the liquid phase and the area above is the solid phase. The interval between the grain boundaries is taken to be 40 μm (that reported in the previous study[6]). The diffusion coefficient at the grain boundary region is assumed to be greater than the bulk diffusion coefficient by a factor of 10^3. As shown in Figures 7 and 8, although the grain boundary diffusion coefficient is assumed to be such a high value, grain boundary diffusion only slightly influences migration of the liquid-solid interface, and the width of the liquid phase, particularly at the grain boundary region, is decreased. In effect, higher diffusivity at the grain boundary region displaces the liquid-solid interface in a direction opposite that observed in the actual brazing situation (Figure 8).

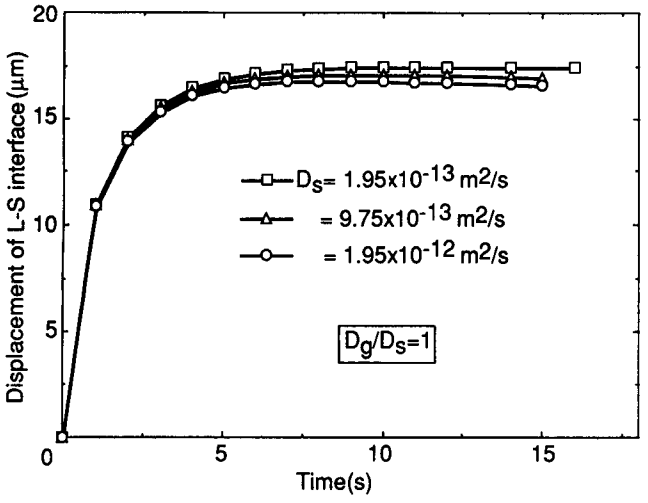

Fig. 5—Relation between the displacement of the liquid-solid interface and the holding time at the brazing temperature when the influence of grain boundaries is ignored.

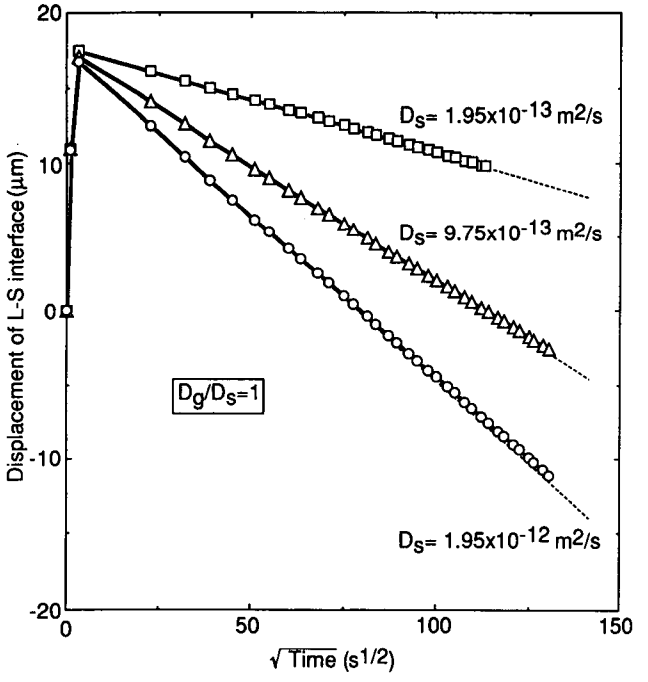

Fig. 6—Relation between the displacement of the liquid-solid interface and the square root of the holding time at the brazing temperature when the influence of grain boundaries is ignored (for different diffusion coefficient values in the solid).

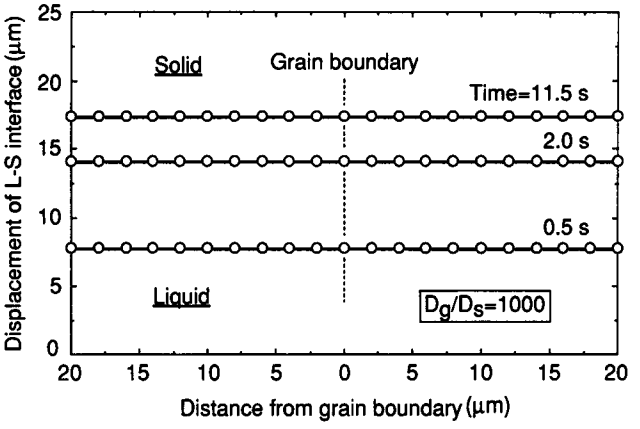

Fig. 7—Evolution of the profile of the liquid-solid interface during the dissolution process when the grain boundary diffusion coefficient is assumed to be 10^3 times as great as that in the bulk material and the influence of the grain boundary energy and the liquid-solid interfacial energy is ignored.

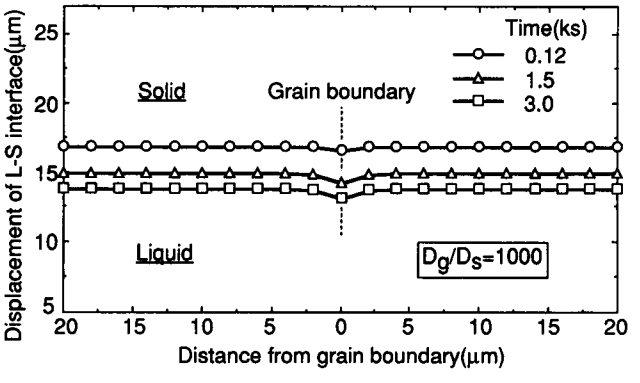

Fig. 8—Evolution of the profile of the liquid-solid interface during the isothermal solidification process following the dissolution process illustrated in Fig. 7.

Figure 9 illustrates the effect of increasing grain boundary diffusivity on migration of the liquid-solid interface at the grain boundary. The width of the liquid phase in regions adjacent to the grain boundary is slightly increased when the grain boundary diffusivity is higher. However, the main influence of higher diffusivity is in decreasing the liquid width at the grain boundary itself. In effect, higher grain boundary diffusivity has negligible influence on movement of the bulk liquid-solid interface and shifts the liquid-solid interface at the grain boundary region in a direction opposite that observed in actual brazed samples (there is no liquid penetration effect).

Because of this, we examined the influence of other factors, namely, the balance between the grain boundary energy and the liquid-solid interfacial energy, the interfacial energy due to the curvature of the liquid-solid interface, and the diffusional flow along the liquid-solid interface. The profiles of the liquid-solid interface under the influence of these factors are shown in Figures 10 and 11. In these results, the grain boundary energy, E_g, is that reported as the energy of a large angle random grain boundary (0.848 J/m^2[122]), the liquid-solid interfacial energy, E_s, is assumed to be $(E_g/\sqrt{3})$, and no increase in solute diffusivity at the grain boundary region exists ($D_g = D_s$).

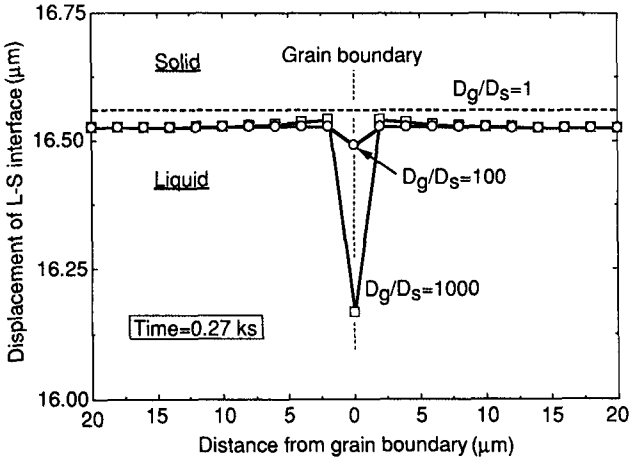

Fig. 9—Effect of the grain boundary diffusivity on the profile of the liquid-solid interface during isothermal solidification.

As shown in Figure 10, the liquid-solid interface is almost planar during the dissolution process and liquid penetration at the grain boundary region is only apparent at the end of the dissolution process. As shown in Figure 11, liquid penetration at the grain boundary becomes more pronounced as the holding time increases during isothermal solidification. The penetration depth at the grain boundary region increases by more than 10 μm, large enough to be observed using conventional optical and scanning electron microscopy. These indications are in accord with the experimental results observed in Reference 6, namely, that the liquid penetration is not observed during the dissolution stage but becomes much more pronounced with increasing holding time at the brazing temperature during the solidification stage. The horizontal dotted lines in Figure 11 show the calculated displacements of the liquid-solid interface when the effects of grain boundary-related factors are neglected. It is clear that the width of the liquid phase in regions far from the grain boundary (represented by the width at the axis of symmetry) is smaller when the effects due to grain boundary energy and liquid-solid interfacial energy are taken into account. It follows that the isothermal solidification process in the bulk region is accelerated when the effects of grain boundary energy and liquid-solid interfacial energy are taken into account. However, although the calculated liquid penetration depth is comparable with Kokawa *et al.*'s test results,[6] the observed difference in the widths of the bulk liquid during TLP brazing of fine-grained and coarse-grained nickel was significantly larger than in our calculated results.

The influence of grain boundary energy on liquid penetration at the grain boundary region is shown in Figure 12. In this figure, the liquid-solid interfacial energy is maintained at a value of 0.424 J/m^2 and the grain boundary energy is varied from 0.424 to 0.848 J/m^2. It

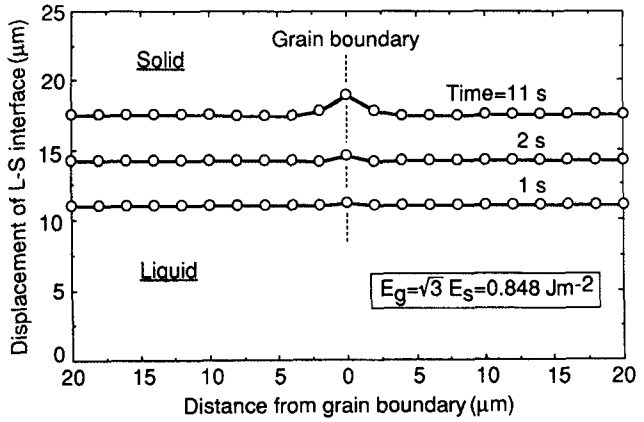

Fig. 10—Evolution of the profile of the liquid-solid interface during the dissolution process when the influence of the grain boundary energy and the liquid-solid interfacial energy is considered. (The diffusion coefficient in the bulk material and at the grain boundary region are identical in this case.)

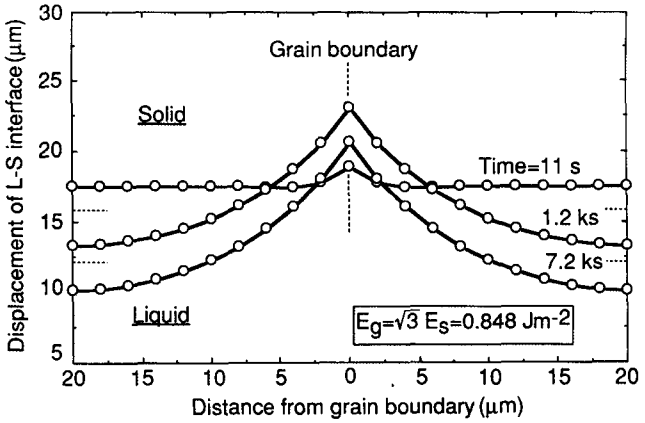

Fig. 11—Evolution of the profile of the liquid-solid interface during isothermal solidification following the dissolution process illustrated in Fig. 10. (The horizontal broken lines in this figure indicate the displacement of the liquid-solid interface when the effect of grain boundary-related factors is neglected.)

is apparent from Figure 12 that the penetration depth increases and the angle at which the liquid-solid interface intersects the grain boundary becomes sharper when the grain boundary energy is increased. Kokawa *et al.*[6] observed that liquid penetration at large angle random grain boundaries was much more pronounced than that occurring at ordered grain boundaries (including small angle grain boundaries and twin boundaries). Since a large angle random grain boundary has higher energy than an ordered grain boundary, the calculated results shown in Figure 12 correspond well with Kokawa *et al.*'s experimental observations.

Liquid penetration at the grain boundary region is also influenced strongly by the liquid-solid interfacial energy (Figure 13) and is more pronounced when the liquid-solid interfacial energy decreases.

In our results, the effect of increasing diffusion along the liquid-solid interface (by varying the diffusion coefficient from zero to the diffusion coefficient value in the liquid phase) only slightly enhanced liquid penetration at the grain boundary region.

It has already been confirmed in Figure 6 that increasing solute diffusivity in the solid accelerates the isothermal solidification process. However, increasing solute diffusivity in the solid has little influence on the shape of the liquid-solid interface at the grain boundary region (it slightly decreases liquid penetration).

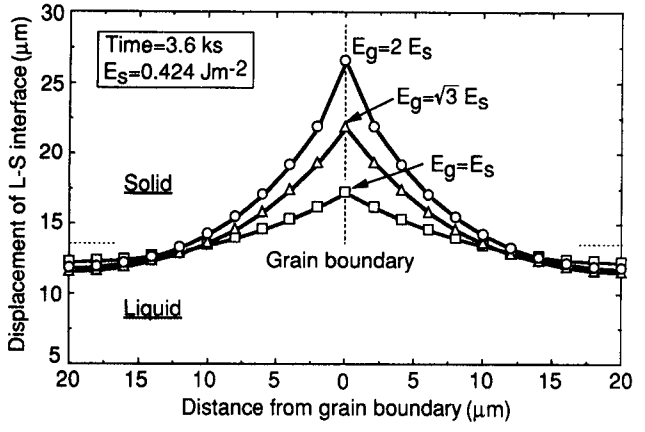

Fig. 12—Effect of the grain boundary energy on the profile of the liquid-solid interface during the isothermal solidification.

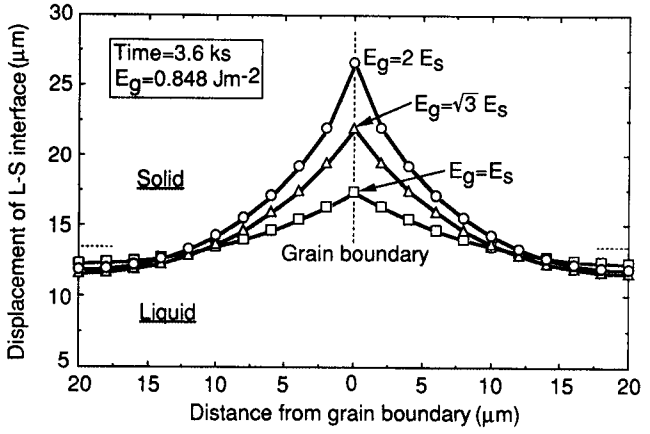

Fig. 13—Effect of the liquid-solid interfacial energy on the profile of the liquid-solid interface during isothermal solidification.

V. DISCUSSION

A. *Kinetics of the Isothermal Solidification Process*

As can be seen from the results presented in Figures 5 and 6 (where grain boundary-related effects are neglected), the isothermal solidification process requires a much longer period than the dissolution process, and therefore, this may be considered to be the major factor which controls the completion time for TLP brazing. During isothermal solidification, the kinetics of migration of the liquid-solid interface are only slightly influenced by the diffusion coefficient in the liquid phase and can be expressed as a linear function of $(\text{time})^{1/2}$, as shown in Figure 6. This suggests that migration of the liquid-solid interface during the isothermal solidification process is governed by diffusion in the solid phase and that diffusion in the liquid is less important, since the composition of the liquid phase becomes uniform. In such a situation, migration of the liquid-solid interface can be approximately evaluated using the model illustrated in Figure 14. In this case, the concentration in the liquid phase is maintained at the liquidus concentration, C_l^0, and migration of the interface is dependent only on diffusion in the solid phase. The analytical solution of this problem is given by the following equations:[23]

$$Y' = Y - Y_{\max} = 2 \cdot \beta \cdot \sqrt{t} \qquad [29]$$

where $Y_{\max}$ is the maximum value of displacement Y and β is determined by the following equation:

$$\frac{\exp(-\beta^2/D_s)}{1 - \operatorname{erf}(\beta/\sqrt{D_s})} \cdot \frac{\sqrt{D_s}}{\beta} - \sqrt{\pi} \cdot \frac{C_s^0 - C_l^0}{C_s^0} = 0 \qquad [30]$$

The dotted lines in Figure 6 show the relation given by Eqs. [29] and [30], and there is good agreement with the finite difference analysis results. Therefore, if the effect of grain boundary regions is neglected, the migration of the liquid-solid interface during the isothermal solidification process can be well approximated by Eqs. [29]

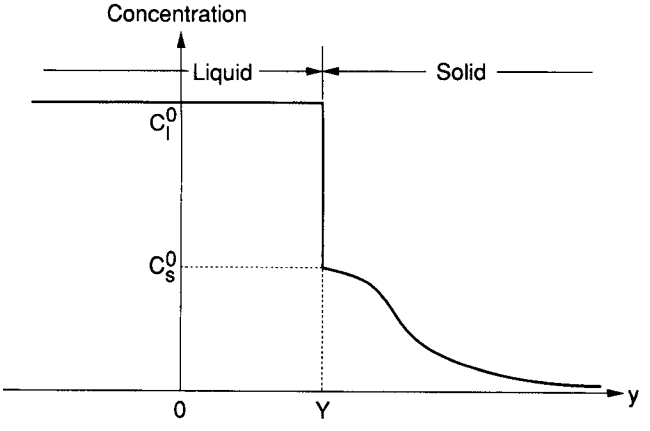

Fig. 14—Schematic showing the model for approximate estimating the migration kinetics of the liquid-solid interface during isothermal solidification.

and [30], although it is necessary to estimate Y_{max} using finite difference modeling. The excellent agreement between the calculated results and the finite difference analysis results supports the validity of our treatment of liquid-solid interface migration.

B. *Effects of the Grain Boundary Diffusion on the Migration of the Liquid-Solid Interface*

If the exact profile of the liquid-solid interface at the grain boundary region and its vicinity is to be estimated, we should solve the problem using the finite difference expression for Eq. [12] instead of Eq. [23] which gives the average composition in the vicinity of the grain boundary. However, the stability of the solution obtained using the finite difference expression for Eq. [12] is not satisfied unless a grid size ε comparable with the width of the grain boundary region is employed. The use of a grid size ε as small as the grain boundary region involves extremely long calculation times to obtain results comparable with experimental values (assuming that we employ the explicit finite difference method).

We believe that the results presented in this article, although they are based on the average composition at the grain boundary region, provide meaningful trends concerning the effect of grain boundary diffusion on migration of the liquid-solid interface. The results which indicate that isothermal solidification at the grain boundary region is preferentially accelerated by high diffusivity at the grain boundary region can be explained by considering that an increase in D_g reduces the term $(\partial Y/\partial t)$ given in Eq. [11] (for $(\partial C_l/\partial y)_{y=Y} < 0$ and $(\partial C_s/\partial y)_{y=Y} < 0$). Since $(\partial Y/\partial t)$ is the rate of increase in liquid width, it follows that a decrease in $(\partial Y/\partial t)$ is associated with increased growth of solid at the grain boundary region during isothermal solidification. This is consistent with Seith's suggestion[24] that the growth rate of phases formed during reactive diffusion increases when the solute diffusivity increases. Consequently, solid grows at a faster rate at the grain boundary region, because the diffusivity is higher than in the bulk material.

The slight increase in the liquid width immediately adjacent to the grain boundary region (Figure 9) occurs, since the phosphorus concentration in solid material near the grain boundary is increased due to higher diffusivity at the grain boundary region. Higher phosphorus concentration in this region promotes liquid formation. In our results, the increase in liquid width caused by this higher phosphorus concentration is quite small (<1 μm), even when the D_g value is assumed to be as much as five orders of magnitude higher than that in the bulk solid.

Although the average composition at the grain boundary region has been calculated in our work, we believe that the general trends indicated in this article will remain unchanged even if more accurate calculations are made (*e.g.*, using implicit finite difference or finite element analysis methods). Consequently, higher grain boundary solute diffusivity *by itself* cannot explain the liquid penetration effect which was observed in actual TLP brazed samples.

C. *The Balance between Grain Boundary Energy and the Liquid-Solid Interfacial Energy*

Figures 11 through 13 indicate that liquid penetration is produced at grain boundary regions to a depth of around 10 μm when factors, such as (a) the balance between the grain boundary energy and liquid-solid interfacial energy, (b) the interfacial energy due to the curvature of the liquid-solid interface, and (c) the diffusional flow along the liquid-solid interface, are taken into account. These factors also accelerate isothermal solidification in bulk regions away from the grain boundary, as shown in Figures 11 through 13. Although the term $(\Delta\mu/RT)$ in Eqs. [15], [16], [18], and [19] changes the liquidus and solidus compositions only by a factor of 10^{-3}, the calculated penetration depth compares well with the experimental values observed in a previous article.[6] However, the combined influence of factors (a) through (c) is still not large enough to explain the large difference between the isothermal solidification rates in fine-grained and coarse-grained nickel-base metal (as reported in Reference 6).

The isothermal solidification process is slightly accelerated when high grain boundary diffusivity values are assumed (Figure 9). However, the large difference between the isothermal completion rates when brazing fine- and coarse-grained nickel-base materials (in Reference 6) can only be explained if extremely high diffusivity values are assumed. It follows that the results of this study provide a qualitative rather than a quantitative analysis of the individual effects which control isothermal solidification during TLP brazing of nickel using Ni-11 wt pct P filler metal.

It is well known that the grain boundary energy is affected by solute segregation at the grain boundary.[25] For example, in the Fe-P binary system at 1623 K, the energy of large angle random grain boundaries is reduced from 0.8 to 0.55 Jm^{-2} by the addition of 0.3 wt pct P.[25] Similarly, the grain boundary energy of Ni may also be reduced by the addition of phosphorus. The phosphorus content at the liquid-solid interface is controlled by the liquidus and solidus lines and, therefore, remains constant throughout dissolution and isothermal solidification. Consequently, the energy of the grain boundary at the point of intersection with the liquid-solid interface may be regarded as constant, even if the phosphorus segregation at the grain boundary region occurs. It follows that our calculations, where the grain boundary energy is considered constant (Figures 11 through 13), may apply to the situation where phosphorus segregation influences the grain boundary energy.

In our results, the ratio of the grain boundary energy and the liquid-solid interfacial energy, E_g/E_s, is the major factor which controls the liquid penetration depth at the grain boundary region rather than the value of grain boundary energy itself. A decrease in grain boundary energy will slow down the development of liquid penetration and only slightly decrease the penetration depth (a 50 pct decrease in grain boundary energy will reduce the penetration depth by a few percent for the same E_g/E_s ratio, see the curves for $E_g/E_s = 1$ in Figures 12 and 13). It follows that liquid penetration at grain boundaries

can be explained qualitatively by factors (a) through (c) (the effects of grain boundary energy and the liquid-solid interfacial energy), even when the grain boundary energy is reduced considerably because of phosphorus segregation.

VI. CONCLUSIONS

The effects of grain boundary regions on liquid-solid interface migration during TLP brazing of Ni using Ni-11 wt pct P filler metal were calculated numerically to explain the higher isothermal solidification rates which were observed during brazing of fine-grained nickel-base metal.[6] The 2-D finite difference model developed in this study considered the situation where the grain boundary intersected the liquid-solid interface at right angles. In addition to solute diffusion in the liquid and solid phases, the numerical calculations allowed for the following factors:

1. increased solute diffusivity at the grain boundary region;
2. the balance between the grain boundary energy and the liquid-solid interfacial energy;
3. the interfacial energy due to the curvature of the liquid-solid interface; and
4. diffusional flow along the liquid-solid interface.

Although higher diffusivity at the grain boundary region accelerates the isothermal solidification process in the bulk region, this effect is very small and cannot explain the experimental test results (where the rate of isothermal solidification is much faster during TLP brazing of fine-grained nickel-base metal). In addition, high diffusivity at the grain boundary region moves the liquid-solid interface in a direction opposite that observed in actual brazed samples. When factors 2 through 4 are taken into account, liquid penetration at the grain boundary regions is comparable with that observed in actual brazed samples. Also, the dependence of liquid penetration depth, both on holding time at the brazing temperature and on grain boundary energy, follows the same trends as in the experimental test results. Factors 2 through 4 also accelerate the isothermal solidification process in bulk regions away from the grain boundary; this is again in qualitative agreement with the experimental test results.

ACKNOWLEDGMENTS

The authors wish to acknowledge the financial support provided by the Ontario Center for Materials Research and the Welding Research Council in New York, NY.

REFERENCES

1. D.S. Duvall, W.A. Owczarski, and D.F. Paulonis: *Weld. J.*, 1974, vol. 53, pp. 203-14.
2. Y. Nakao, K. Nishimoto, K. Shinozaki, C.H. Kang, and Y. Hori: *Q. J. Jpn. Weld. Soc.*, 1988, vol. 6, pp. 519-26.
3. H. Ikawa, Y. Nakao, and T. Isai: *Trans. Jpn. Weld. Soc.*, 1979, vol. 10, pp. 24-29.
4. H. Nakagawa, C.H. Lee, and T.H. North: *Metall. Trans. A*, 1991, vol. 22A, pp. 543-55.
5. I. Tuah-Poku, M. Dollar, and T.B. Massalski: *Metall. Trans. A*, 1988, vol. 19A, pp. 675-86.
6. H. Kokawa, C.H. Lee, and T.H. North: *Metall. Trans. A*, 1991, vol. 22A, pp. 1627-31.
7. K. Nishiguchi, Y. Takahashi, and A. Seo: *Q. J. Jpn. Weld. Soc.*, 1990, vol. 8, pp. 336-42.
8. T.H. North, K. Ikeuchi, Y. Zhou, and H. Kokawa: *Metal Science of Joining Symp.*, TMS Fall Meeting, Cincinnati, OH, Oct. 1991.
9. W.W. Mullins: *J. Appl. Phys.*, 1957, vol. 28, pp. 333-39.
10. W.W. Mullins: *Trans. TMS-AIME*, 1960, vol. 218, pp. 354-61.
11. C.S. Smith: *Trans. ASM*, 1953, vol. 45, pp. 533-75.
12. C.A. Steidel, Che-Yu Li, and C.W. Spencer: *Trans. TMS-AIME*, 1964, vol. 230, pp. 84-88.
13. H.J. Vogel and L. Ratke: *Acta Metall. Mater.*, 1991, vol. 39, pp. 641-49.
14. A. Lazaridis: *Int. J. Heat Mass Transfer*, 1970, vol. 13, pp. 1459-77.
15. D.G. McCartney and J.D. Hunt: *Metall. Trans. A*, 1984, vol. 15A, pp. 983-94.
16. D.L. Sikarskie and B.A. Boley: *Int. J. Solids Struct.*, 1965, vol. 1, pp. 207-34.
17. P.D. Patel: *J. AIAA*, 1968, vol. 6, p. 2454.
18. J.C. Fisher: *J. Appl. Phys.*, 1951, vol. 22, pp. 74-77.
19. R.A. Swalin: *Thermodynamics of Solids*, John Wiley & Sons, Inc., New York, NY, 1962, pp. 180-87.
20. P.G. Shewmon: in *Physical Metallurgy*, R.W. Cahn, ed., North-Holland Publishing Co., New York, NY, 1970, pp. 303-06.
21. J. Crank: *The Mathematics of Diffusion*, Clarendon Press, Oxford, 1975, p. 273.
22. L.E. Murr: *Interfacial Phenomena in Metals and Alloys*, Addison-Wesley Publishing Company, Reading, MA, 1975, pp. 130-35.
23. P.V. Danckwerts: *Trans. Faraday Soc.*, 1950, vol. 46, pp. 701-12.
24. W. Seith: *Diffusion in Metallen*, Springer-Verlag, Berlin, 1955, pp. 157-81.
25. E.D. Hondros: *Proc. R. Soc., Ser. A*, 1965, vol. 286, pp. 479-98.